

Crossing the Hopf Bifurcation in a Live Predator-Prey System

Gregor F. Fussmann,^{1*} Stephen P. Ellner,^{1,2} Kyle W. Shertzer,² Nelson G. Hairston Jr.¹

Population biologists have long been interested in the oscillations in population size displayed by many organisms in the field and laboratory. A wide range of deterministic mathematical models predict that these fluctuations can be generated internally by nonlinear interactions among species and, if correct, would provide important insights for understanding and predicting the dynamics of interacting populations. We studied the dynamical behavior of a two-species aquatic laboratory community encompassing the interactions between a demographically structured herbivore population, a primary producer, and a mineral resource, yet still amenable to description and parameterization using a mathematical model. The qualitative dynamical behavior of our experimental system, that is, cycles, equilibria, and extinction, is highly predictable by a simple nonlinear model.

Nonlinear mathematical models of interacting populations often predict exceedingly complicated dynamics even when system complexity is low (two or three species) (1–3). Their relevance to field communities has, however, often been questioned. Although population cycles have been shown to occur in both the field [see, e.g., (4)] and in laboratory cultures [see, e.g., (5)], reconciling the predictions of mathematical models with the nonequilibrium dynamics of experimental communities has proved challenging. Studies on microbial populations have come closest to meeting this goal (6–8) and have provided valuable evidence that simple mechanistic rules determine the dynamical state of interacting populations. In this study, we demonstrate that this finding does not hinge on the simplicity of the single-celled organisms (bacteria and protists) used and the short duration of the experiments (several hundred hours), but holds for the communities of demographically structured populations that are more often the subject of study in the wild. Our experimental community includes an age-structured, metazoan population that can be maintained at the same dynamical state for more than 100 days. Rigorous experimental analyses that have looked into the demographic causes of population cycles have, to date, either been confined to a single-species system (9) or have used assemblages of multiple species too complex for a species-based mathematical formulation (10). Here, we combine theoretical and empirical approaches to demonstrate that a few simple mechanistic processes underlie com-

plex multispecies dynamics and that a correspondingly simple model is a sound tool for investigating community properties.

Our system is a predator-prey food chain that consists of planktonic rotifers, *Brachionus calyciflorus*, feeding on unicellular green algae, *Chlorella vulgaris*. Nitrogen is the resource that limits the algal growth. Two earlier studies have demonstrated the potential for predator-prey oscillations in this system (11, 12). We cultured the two species together in continuous flow-through systems, in chemostats (11–13) and monitored their population dynamics under different experimental conditions (14). The two key parameters that can be experimentally varied in a chemostat setup are the resource concentration of the inflow medium N_i and the dilution rate δ (the fraction of the volume of the system replaced daily). The chemostat system can be nutritionally enriched by increasing either δ or N_i . Although both methods lead to increased nutrient supply, high δ values additionally impose an increased mortality on the organisms through washout.

The mathematical model is a system of four differential equations:

$$dN/dt = \delta(N_i - N) - F_C(N)C \quad (1)$$

$$dC/dt = F_C(N)C - F_B(C)B/\epsilon - \delta C \quad (2)$$

$$dR/dt = F_B(C)R - (\delta + m + \lambda)R \quad (3)$$

$$dB/dt = F_B(C)R - (\delta + m)B \quad (4)$$

with $F_C(N) = b_C N / (K_C + N)$; $F_B(C) = b_B C / (K_B + C)$.

In this model, N is the concentration of nitrogen, C the concentration of *Chlorella*, R the concentration of reproducing *Brachionus*, and B the total concentration of *Brachionus* (15). Our model is based on continuous, asexual reproduction of *Chlorella* and *Brachionus*. Nitrogen concentration in the chemostat determines the birth rate of the *Chlorella* population, whereas the

concentration of *Chlorella* determines the birth rate of the *Brachionus* population. Both follow Holling type II (16) response curves (F_C , F_B); the uptake function of *Brachionus* is F_B/ϵ , with ϵ being the assimilation efficiency of *Brachionus*. About 90% of the algal nitrogen that rotifers do not assimilate is released as particulate organic nitrogen (17), which is assumed to wash out of the chemostat before any mineralization occurs; the small amount of inorganic nitrogen excreted by the rotifers is omitted for simplicity. Nitrogen is continuously added to the system at the dilution rate δ ; all components are removed from the system at the same δ . N_i is the nitrogen concentration in the inflow medium; b_C and b_B are the maximum birth rates of *Chlorella* and *Brachionus*; K_C and K_B are the half-saturation constants of *Chlorella* and *Brachionus*. Demographic structure is represented by the mortality of *Brachionus*, m , and the decay of fecundity of *Brachionus*, λ . δ and N_i are adjustable parameters of the chemostat system. We derived all other parameter values from our own chemostat system or used published sources on *Chlorella* and *Brachionus* (18).

Our model differs in two important ways from standard predator-prey models. First, as a consequence of the chemostat setup, we include the inorganic resource as a state variable. This allows accurate modeling of the uptake dynamics of the algal population and is preferable to the common practice of positing logistic growth for the primary producer (2, 3). Second, we include predator mortality—as in (19)—and senescence rate, which substantially alter the dynamics at low δ . Commonly, δ is the only loss term for organisms in chemostat models (20, 21).

Our model predicts one of three behaviors: extinction of the predator or of both predator and prey, coexistence at an equilibrium, or coexistence on limit cycles. The dynamics predicted depend on the values of N_i and δ and show distinct transitions between these types of behavior (Fig. 1A). Low nutrient supply, i.e., either low δ or low N_i , keeps the two species at an equilibrium (19), unless the nutrient input is too low to sustain the predator population or both the predator and the prey populations. Enrichment can destabilize the system and cause it to switch to a limit cycle. The effect of further enrichment depends on whether N_i or δ is altered. Increasing δ causes the system to switch back to equilibrium. Increasing N_i , however, leads to extreme oscillations. Although the mathematical model allows the populations to recover from infinitesimal numbers, we—more realistically—regard populations below a threshold density of one individual per chemostat as unable to survive. Region d in Fig. 1A indicates where such extreme oscillations occur in the model, and we predict extinction for these parameter values.

According to the model and common sense, rotifers and algae only survive in the chemostat

¹Department of Ecology and Evolutionary Biology, Corson Hall, Cornell University, Ithaca, NY 14853, USA. ²Biomathematics Program, Department of Statistics, North Carolina State University, Raleigh, NC 27695–8203, USA.

*To whom correspondence should be addressed. E-mail: GFF1@cornell.edu

REPORTS

if their birth rates are greater than their death rates. At low δ , old rotifers accumulate, and the proportion of the rotifer population that contributes to reproduction drops. Under this condition, if N_i is sufficiently high, primary production can compensate for the reproducing rotifers' total mortality ($\lambda + m + \delta$), and algae and rotifers coexist at an equilibrium. At higher δ , the age structure shifts toward younger individuals, nutrient supply and algal production are sufficiently high to allow high rotifer birth rates, and, in this case, rotifers and algae coexist at an equilibrium that is characterized by high reproduction and rapid turnover. In our model, starting at any combination of δ and N_i yielding equilibrium conditions (Fig. 1A, region b) and increasing N_i eventually leads to the coexistence of rotifers and algae on a limit cycle. This destabilizing effect of enrichment is well established in theoretical population biology as the "paradox of enrichment" (1). The critical point at which the equilibrium ceases to exist and the limit cycle is born marks a "supercritical Hopf bifurcation" (22). Because we analyze our system in two parameter dimensions, a curve separates the regions of equilibria and limit cycles (Fig. 1A, regions b and c). Crossing this curve results in a Hopf bifurcation.

We ran 18 chemostat trials with predator and prey populations at 14 different dilution rates and two different nitrogen concentrations (Fig. 1A). One set of trials represents a transect across the two-dimensional parameter space at constant $N_i = 80 \mu\text{mol/liter}$ with δ varying between 0.04 and 1.37 per day (Fig. 1B). Four trials were run at elevated $N_i = 514 \mu\text{mol/liter}$ and an average δ of 0.44 per day. In these four trials, we consistently observed extinction of *Brachionus* after *Chlorella* had been grazed down to very low densities (Fig. 2A). All our trials at low N_i resulted in the coexistence of *Brachionus* and *Chlorella* either at an equilibrium or on limit cycles (Fig. 2, B to E). At intermediate δ , the two populations oscillated, whereas at very low and very high δ , they remained at equilibrium. This was true whether we kept δ constant throughout one trial or switched it during the trial, thereby transferring the dynamics from equilibrium to oscillations (Fig. 2D).

To summarize the dynamics of all chemostat runs at low N_i , we computed the coefficient of variation (CV) of *Chlorella* and *Brachionus* densities for each trial. The CV ought to be zero for all state variables of a noise-free system at equilibrium, but greater than zero if the system oscillates. We plotted CV (23) as a function of δ (Fig. 3) and recovered the dynamical behavior predicted by the model. There are three distinct groups of trials: one at intermediate δ with $\text{CV} > 30\%$ (oscillating populations), the other two with $\text{CV} < 18\%$, either at high or low δ . These two groups contain only populations at equilibrium, and we attribute the remaining

CV to noise associated with the experimental system.

According to our experiments, the two Hopf bifurcations occur at 0.32 per day $< \delta < 0.64$ per day and at $\delta \approx 1.16$ per day. We were able to separate continuous regions of oscillations and equilibria along the δ gradient. Conflicting evidence at $\delta \approx 1.16$ per day (i.e., one trial with oscillations, one at equilibrium) corroborates our localization of the second bifurcation. In its neighborhood, the

dynamical behavior changes rapidly, and slight differences (e.g., in temperature or illumination) between two chemostats run at identical δ may cause the system to settle on either oscillations or equilibrium. We note that both bifurcation points we observed are shifted toward slightly higher dilution rates than the model predicts (Fig. 1B, region 3), probably because of subtle inaccuracies in the parameter estimation.

We conclude that our model reliably ex-

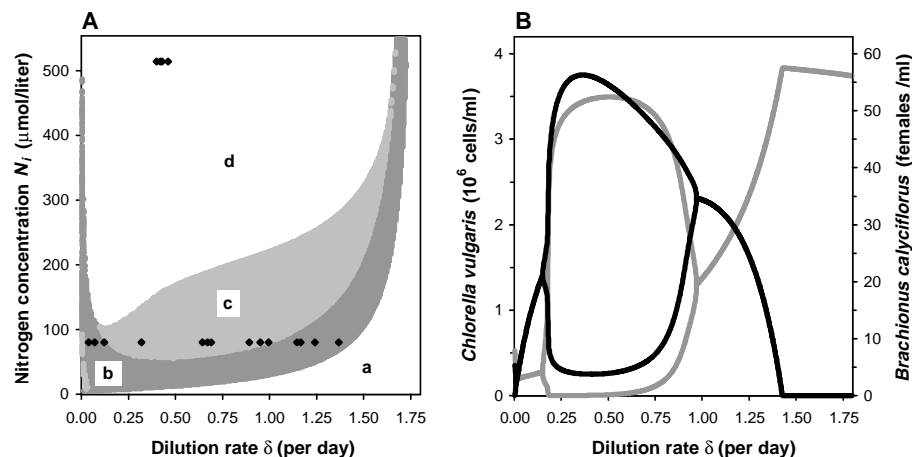


Fig. 1. Predictions of the mathematical model. (A) Theoretical dynamic states of the chemostat predator-prey system as a function of nitrogen inflow concentration (N_i) and dilution rate (δ). Plotted are the results of numerical simulations on a 256×512 grid in the (δ, N_i) parameter plane. Region a: Extinction of the predator alone or of both predator and prey together. Region b: Coexistence at an equilibrium. Region c: Coexistence on a stable limit cycle. Region d: Extinction due to extreme cycles (see text). Points indicate the 18 combinations of N_i and δ for which we ran chemostat trials in this study. (B) Bifurcation diagram showing the maxima and minima of predator (*B. calyciflorus*, black line) and prey (*C. vulgaris*, gray line) concentration for the chemostat system across the range of 0 per day $< \delta < 1.8$ per day, and at constant $N_i = 80 \mu\text{mol/liter}$.

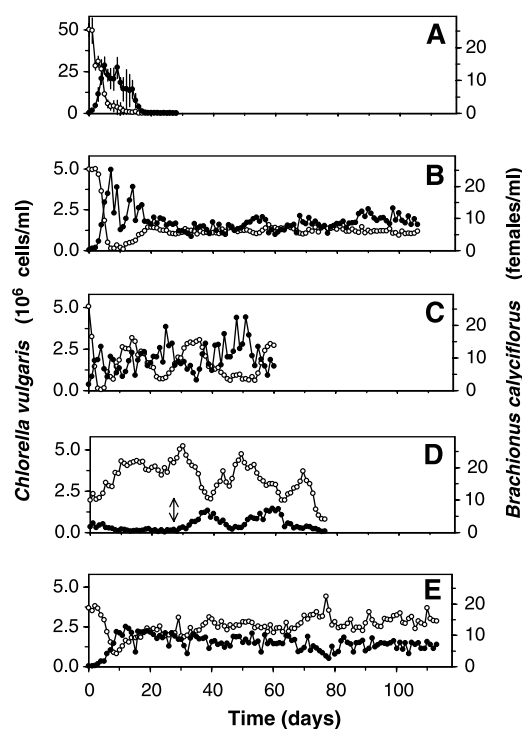


Fig. 2. Example experimental results showing extinction, equilibria, and population cycles at different values of chemostat dilution rate (δ) and nitrogen inflow concentration (N_i). Population dynamics of *B. calyciflorus* (predator, black symbols) and *C. vulgaris* (prey, open symbols). Straight lines connect daily sampling results. (A) Extinction of the predator at high $N_i = 514 \mu\text{mol/liter}$ and intermediate $\delta = 0.44$ per day. Values are means \pm SD of four synchronous trials. (B to E) Examples of trials at low $N_i = 80 \mu\text{mol/liter}$. (B) Equilibrium at low $\delta = 0.04$ per day. (C) Cycles at intermediate $\delta = 0.64$ per day. (D) Transition from equilibrium to cycles; $\delta = 1.15$ per day on left side of the arrow, $\delta = 0.95$ per day on right side of the arrow. (E) Equilibrium at high $\delta = 1.24$ per day. Note different scale for *C. vulgaris* in (A).

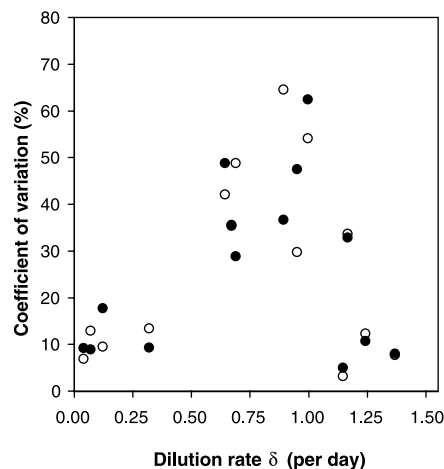


Fig. 3. Relative stability of experimental predator-prey chemostat cultures. Coefficient of variation (23) of time series (day 20 to end of trial) for all chemostat trials at $N_i = 80 \mu\text{mol/liter}$. Low CV indicates populations at equilibrium ($CV > 0$ because of noise), high CV indicates fluctuating populations. *Brachionus calyciflorus* (predator, black symbols) and *C. vulgaris* (prey, open symbols).

plains the overall dynamical behavior of the nitrogen-*Chlorella-Brachionus* system; a simple laboratory culture system containing populations of real predators and prey exhibits the oscillatory dynamics predicted by a mathematical model. This model is of the same type that has led theoreticians to posit that fluctuations in natural populations may be internally driven (24). However, the model does not correctly predict some of the quantitative characteristics: the observed cycle periods are too long, and the positions of the predator minima and prey maxima are too close together relative to prediction. This suggests that some additional mechanism, not represented in our model (e.g., variable algal quality), comes into play only when the populations are undergoing large-amplitude cycles.

The rotifer-algal chemostat system has allowed us to study the conditions under which predator-prey cycles arise. It now provides an opportunity to explore the occurrence of more complex dynamics such as deterministic chaos (20–22), cyclic predator-prey coevolution (25), and evolutionary responses that might reduce the likelihood of complex dynamics (26).

References and Notes

1. M. L. Rosenzweig, *Science* **171**, 385 (1971).
2. A. Hastings, T. Powell, *Ecology* **72**, 896 (1991).
3. K. McCann, A. Hastings, G. R. Huxel, *Nature* **395**, 794 (1998).
4. C. S. Elton, M. Nicholson, *J. Anim. Ecol.* **11**, 215 (1942).
5. L. S. Luckinbill, *Ecology* **54**, 1320 (1973).
6. J. L. Jost, J. F. Drake, A. G. Fredrickson, H. M. Tsuchiya, *J. Bacteriol.* **113**, 834 (1973).
7. J. L. Jost, J. F. Drake, H. M. Tsuchiya, A. G. Fredrickson, *J. Theor. Biol.* **41**, 461 (1973).

8. V. E. Dent, M. J. Bazin, P. T. Saunders, *Arch. Microbiol.* **109**, 187 (1976).
9. R. F. Constantino, J. M. Cushing, B. Dennis, R. A. Desharnais, *Nature* **375**, 227 (1995).
10. E. McCauley, R. M. Nisbet, W. W. Murdoch, A. M. DeRoos, W. S. C. Gurney, *Nature* **402**, 653 (1999).
11. U. Halbach, *Oecologia* **4**, 176 (1970).
12. M. E. Boraas, *Am. Soc. Limnol. Oceanogr. Spec. Symp.* **3**, 173 (1980).
13. We established cultures of *C. vulgaris* (UTEX no. 26) and *B. calyciflorus* in 380-ml glass chemostats at $25^\circ \pm 0.3^\circ\text{C}$ and constant fluorescent illumination at $120 \pm 20 \mu\text{E/m}^2$ per second. A continuous flow of sterile medium was pumped through the chemostats; sterile air was bubbled continuously both to prevent CO_2 limitation of the algae and to enhance mixing. We removed algal growth from the inner walls of the vessels daily. Our medium ($\text{pH} = 6.8 \pm 0.4$) contained nitrate at concentrations that limited algal growth, plus nonlimiting concentrations of other nutrients, trace metals, and vitamins.
14. Trials were started by adding *B. calyciflorus* to a chemostat culture of *C. vulgaris* and lasted between 16 and 120 days. We sampled daily (using hypodermic syringes; 0.457-mm needle) through ports near bottom and top of each chemostat. Entire samples were counted for rotifers under a dissecting microscope. Samples of algae preserved in Lugol's solution were counted using either a compound microscope or a particle counter (CASY 1, Schärfe, Germany). We detected no systematic overrepresentation of organisms in either the top or bottom samples. All data on organismal concentrations are means of duplicate samples.
15. Because our data suggest that the rotifers become senescent as they age (fecundity decreases although food uptake remains unchanged), we introduced a fecundity decay rate (λ), and a variable (β) for the total concentration of (reproducing and nonreproducing) rotifers (R includes only reproducing rotifers).
16. C. S. Holling, *Can. Entomol.* **91**, 293 (1959).
17. S. Aoki, A. Hino, *Fisheries Sci.* **62**, 8 (1996).
18. We parameterized our model with $b_c = 3.3$ per day; $K_c = 4.3 \mu\text{mol/liter}$ (27); $b_b = 2.25$ per day; $K_b = 15 \mu\text{mol/liter}$ [from nonlinear regression of data on functional response in (28)]; $m = 0.055$ per day; $\lambda = 0.4$ per day; $\epsilon = 0.25$ (17). We took b_c to be the
- highest δ at which *Chlorella* can maintain a stable population in the chemostat in the absence of rotifers and estimated b_b from data for exponentially growing *Brachionus* under high algal density. We used counts of dead rotifers from chemostat cultures to determine m . Counts of subitaneous eggs per rotifer provided estimates for fecundity and λ . N , C , R , and B are modeled as moles of nitrogen and then converted to numbers of organisms [$1 \mu\text{mol/liter}$ of *Chlorella* = 5×10^4 cells per milliliter (12); $1 \mu\text{mol/liter}$ of *Brachionus* = 5 females per milliliter (12)].
19. R. M. Nisbet, A. Cunningham, W. S. C. Gurney, *Bio-tech. Bioeng.* **25**, 301 (1983).
20. M. Kot, G. S. Saylor, T. W. Schultz, *Bull. Math. Biol.* **54**, 619 (1992).
21. A. Gragani, O. De Feo, S. Rinaldi, *Bull. Math. Biol.* **60**, 703 (1998).
22. S. H. Strogatz, *Nonlinear Dynamics and Chaos* (Addison-Wesley, Reading, MD, 1994).
23. To avoid misinterpretation of trials with low *Brachionus* density, CVs were adjusted by subtracting the CV due to measurement error, which was estimated from duplicate measurements (14). On average the CV was reduced to 78% (*Chlorella*) and 59% (*Brachionus*) of its unadjusted value.
24. R. M. May, *Science* **177**, 900 (1972).
25. A. I. Khibnik, A. S. Kondrashov, *Proc. R. Soc. London Ser. B* **264**, 1049 (1997).
26. S. Ellner, P. Turchin, *Am. Nat.* **145**, 343 (1995).
27. R. Tischner, H. Lorenzen, *Planta* **146**, 287 (1979).
28. U. Halbach, G. Halbach-Keup, *Arch. Hydrobiol.* **73**, 273 (1974).
29. M. Boraas and C. Kearns provided advice on chemostat setup and M. Boraas gave us a culture of *B. calyciflorus*. G. Heber performed extensive numerical simulations for Fig. 1 on the AC³ Velocity complex of the Cornell Theory Center (funded by Cornell University, New York State, federal agencies, and corporate partners). R. Babcock, K. Brewer, K. Check, C. Cline, L. Davias, A. Holmes, P. Kalika, M. Kalvestrand, and A. Katholos helped sample and maintain the chemostats. J. Fieberg, C. Kearns, D. Post, L. Puth, J. Rowell, N. Thomson, N. Tisch, C. Webb, and two anonymous referees made helpful comments on the manuscript. Funded by the Andrew Mellon Foundation.

4 August 2000; accepted 18 September 2000

Coherence and Conservation

David J. D. Earn,^{1*} Simon A. Levin,² Pejman Rohani³

A principal aim of current conservation policy is to reduce the impact of habitat fragmentation. Conservation corridors may achieve this goal by facilitating movement among isolated patches, but there is a risk that increased connectivity could synchronize local population fluctuations (causing coherent oscillations) and thereby increase the danger of global extinction. We identify general conditions under which populations can or cannot undergo coherent oscillations, and we relate these conditions to local and global extinction probabilities. We suggest a simple method to explore the potential success of conservation corridors and, more generally, any manipulations of dispersal patterns that aim to protect threatened species or control pests.

There is growing concern about the adverse effects of habitat fragmentation on the long-term viability of endangered species (1).

¹Department of Mathematics and Statistics, McMaster University, Hamilton, Ontario, Canada, L8S 4K1. ²Department of Ecology and Evolutionary Biology, Princeton University, Princeton NJ, 08544 USA. ³Department of Zoology, University of Cambridge, Downing Street, Cambridge CB2 3EJ, UK.

*To whom correspondence should be addressed. E-mail: earn@math.mcmaster.ca

Many studies attempt to evaluate the effects of past actions, to predict the outcomes of further fragmentation, and to promote conservation measures (2, 3).

A critical issue that is often emphasized is synchrony of population dynamics in different habitat patches (4–9). If a population goes extinct in one patch while other patches retain substantial numbers, the classical “rescue effect” can prevent global extinction (7). However, if extinction occurs in all patches